

Imaging

Intracoronary imaging of coronary atherosclerosis: validation for diagnosis, prognosis and treatment

Konstantinos C. Koskinas¹, Giovanni J. Ughi², Stephan Windecker¹,
Guillermo J. Tearney^{3,4}, and Lorenz Räber^{1*}

¹Department of Cardiology, Bern University Hospital, Bern 3010, Switzerland; ²Wellman Center for Photomedicine, Massachusetts General Hospital, Harvard Medical School, Boston, MA, USA; ³Department of Pathology, Harvard Medical School and Massachusetts General Hospital, Boston, MA, USA; and ⁴Harvard-Massachusetts Institute of Technology Health Sciences and Technology, Cambridge, MA, USA

Received 30 July 2015; revised 5 November 2015; accepted 9 November 2015; online publish-ahead-of-print 11 December 2015

While coronary atherosclerosis is a leading cause of mortality, evaluation of coronary lesions was previously limited to either indirect angiographic assessment of the lumen silhouette or *post mortem* investigations. Intracoronary (IC) imaging modalities have been developed that allow for visualization and characterization of coronary atheroma in living patients. Used alone or in combination, these modalities have enhanced our understanding of pathobiological mechanisms of atherosclerosis, identified factors responsible for disease progression, and documented the ability of various medications to reverse the processes of plaque growth and destabilization. These methodologies have established a link between *in vivo* plaque characteristics and subsequent coronary events, thereby improving individual risk stratification, paving the way for risk-tailored systemic therapies and raising the option for pre-emptive interventions. Moreover, IC imaging is increasingly used during coronary interventions to support therapeutic decision-making in angiographically inconclusive disease, guide and optimize procedural results in selected lesion and patient subsets, and unravel mechanisms underlying stent failure. This review aims to summarize current evidence regarding the role of IC imaging for diagnosis and risk stratification of coronary atherosclerosis, and to describe its clinical role for guiding percutaneous coronary interventions. Future perspectives for in-depth plaque characterization using novel techniques and multimodality imaging approaches are also discussed.

Keywords

Intracoronary imaging • Atherosclerosis • Vulnerable plaque • Coronary interventions

Introduction

As coronary artery disease (CAD) remains a leading cause of mortality worldwide,¹ growing interest has focused on characterizing *in vivo* coronary plaque, i.e. the anatomic substrate of clinical CAD manifestations. Coronary angiography depicts a two-dimensional silhouette of the lumen but cannot visualize the arterial vessel wall *per se*. In contrast, intracoronary (IC) imaging modalities allow for direct visualization and characterization of coronary plaque *in vivo*. Intravascular ultrasound (IVUS), the first modality introduced ≈25 years ago,^{2–4} provides tomographic imaging of the vessel wall. The armour of available tools was subsequently enriched with spectral analysis of IVUS radiofrequency (RF) backscattered

signals and optical coherence tomography (OCT) to better characterize plaque morphology, as well as near-infrared spectroscopy (NIRS) to provide compositional (but no structural) information (Table 1). These modalities, along with novel techniques, have broadened our understanding of the natural history of CAD; evaluated the effect of medications on coronary atheroma; and assessed indices of plaque composition that were linked to subsequent cardiovascular events. Moreover, as percutaneous coronary interventions (PCIs) are applied for increasingly complex patient and lesion subsets, IC imaging has shown potential to optimize procedural results and identify mechanisms of stent failure, i.e. restenosis and thrombosis. In this review, we summarize evidence regarding the current role of the main IC imaging modalities (IVUS, OCT,

* Corresponding author. Tel: +41 31 632 0929, Email: lorenz.raeber@insel.ch

Published on behalf of the European Society of Cardiology. All rights reserved. © The Author 2015. For permissions please email: journals.permissions@oup.com.

Table 1 Characteristics of intravascular ultrasound, RF-intravascular ultrasound, optical coherence tomography, and near-infrared spectroscopy for assessing plaque morphology and composition

	IVUS ⁵	RF-IVUS ⁷	NIRS ¹²	OCT ¹¹
General characteristics				
Energy source	Ultrasound	Ultrasound	Near-Infrared light	Infrared light
Pullback speed (mm/s)	0.5–1.0	0.5–1.0	0.5	10–40
Penetration (mm)	8–10	8–10	1–2	1–3
Spatial resolution (µm)	80–120	80–120	n/a	10
Requirement for blood clearance	No	No	No	Yes
Real-time outcome	Yes	No	Yes	Yes
Assessment of native plaque				
Atheroma volume	Yes ^{5,37–40}	Yes ⁷	No	No
Cap thickness	No	No	No	Yes ^{11,19}
Arterial remodelling	Yes ^{5,24}	Yes ^{5,7}	No	No
Calcification	Good ⁵	Good ⁷	–	Modest ¹¹
Lipid pool/necrotic core	–	Good ^{7,8}	Good ^{12,23}	Good ^{11,19}
Imaging of non-superficial lipid-core plaque	–	Yes ⁷	No	No
Macrophage accumulation	No	No	No	Yes ^{11,20}
Neovessels	–	–	–	Modest ¹¹
Assessment of luminal integrity (erosion, rupture, tears)	Modest ⁵	Modest ⁷	–	Good ^{11,17}
Stent/scaffold imaging				
PCI guidance	Yes ^{60,72,73,75,77}	–	–	Yes ^{60,83,85}
In-stent neoatherosclerosis	Poor	Modest ⁹⁷	–	Good ^{97,100}
Underexpansion	Yes ^{69,72,73,75}	n/a	No	Yes ^{81,82,93,94}
Malapposition	Yes ^{69,72,73,75}	n/a	No	Yes ^{81,82,93,94,96}
Strut uncoverage	No	No	No	Yes ^{92,93,95}

IVUS, intravascular ultrasound; n/a, not applicable; NIRS, near-infrared spectroscopy; OCT, optical coherence tomography; RF-IVUS, radiofrequency IVUS.

and NIRS) for diagnosis and risk stratification of CAD, describe their clinical role in PCI guidance, and discuss novel modalities and future perspectives in this field.

Intracoronary imaging modalities for coronary plaque characterization

Based on its ability to delineate the lumen and media-adventitia borders, IVUS allows for identification of plaque in angiographically non-stenotic lesions, quantification of atheroma burden, assessment of arterial remodelling, three-dimensional arterial reconstructions that enable measurement of IC rheology, and evaluation of factors associated with plaque progression or regression when performed serially. Commercially available IVUS probes operate at a frequency of 20 MHz. Higher frequencies (≥ 40 MHz) provide higher resolution and better image quality at the cost of decreased tissue penetration, although recent improvements in transducer design have reduced the negative impact of higher frequencies on penetration.⁵ Grey-scale IVUS cannot directly assess plaque composition; echo-attenuated plaques correlate with fibroatheroma morphology by histology with high specificity but low sensitivity.⁶

Spectral analysis of IVUS-RF backscattered signals allows for characterization of different tissue components. Image analysis systems based on post-processing of backscatter RF data include IVUS-virtual histology (IVUS-VH), iMAP, and integrated backscattered IVUS. Using IVUS-VH, plaque components are classified as necrotic core, fibrofatty tissue, fibrous tissue, or dense calcium; and lesions are classified as pathologic intimal thickening, fibrotic, fibrocalcific plaques, thick- or thin-caped fibroatheroma (TCFA)⁷ (Figure 1). Tissue characterization by IVUS-VH has consistently shown good correlation with histology in human autopsy studies⁸ but not in porcine CAD⁹; in view of these conflicting findings, future scientific research needs to continue focusing on robust validation of existing and novel imaging techniques against histology respecting general requirement, i.e. solid sample sizes, independent imaging core labs and pathology labs.

Optical coherence tomography has 10-fold higher axial (≈ 10 µm) and lateral resolution (≈ 30 µm), but lower penetration depth (1–3 mm) compared with IVUS, such that visualization of the entire depth of a lesion is difficult especially in the presence of lipid-rich tissue where the optical signal is strongly attenuated. Optical coherence tomography has been validated against histology for accurate measurement of cap thickness and tissue composition (fibrous, calcific, lipid-rich/necrotic)¹⁰ and can also detect macrophage

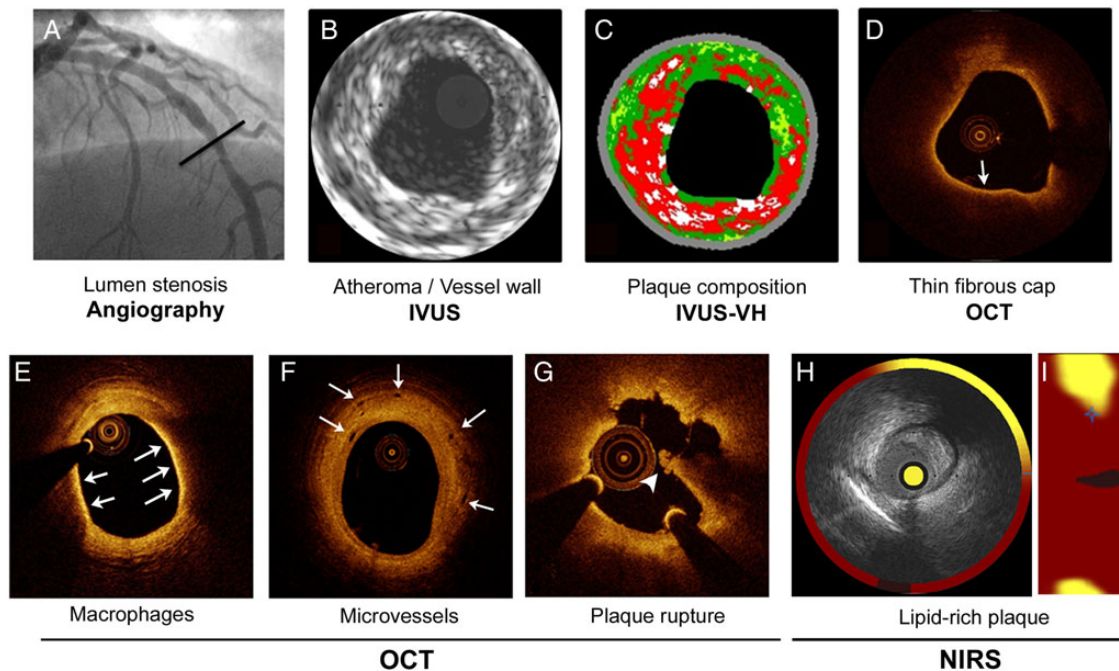


Figure 1 Multimodality imaging of a distal left anterior descending artery lesion by angiography (A), grey-scale intravascular ultrasound (B), intravascular ultrasound-virtual histology (C), and optical coherence tomography (D). The substantial proportion of necrotic core (red colour) with confluence at the luminal site for $>30^\circ$ is consistent with an intravascular ultrasound-virtual histology thin-capped fibroatheroma (C). Optical coherence tomography shows a signal-rich layer and an underlying signal-poor region with high light attenuation, suggestive of lipid/necrotic core with an overlying fibrous cap with minimal thickness $40\ \mu\text{m}$ (arrow), consistent with a thin-capped fibroatheroma (D). In different lesions, optical coherence tomography is capable of visualizing macrophage accumulations forming a line (arrows, E); microvessels (arrows, F); and a ruptured thin-capped fibroatheroma with minor white thrombus on top of the fibrous cap flap (arrowhead, G). Intravascular ultrasound image of a lesion containing a lipid pool, noted by the yellow colour in the surrounding circle (H) and the corresponding chemogram by near-infrared spectroscopy (I).

accumulations, plaque rupture, micro-calcifications, neovascularization, and thrombus¹¹ (Figure 1). Potential limitations include the inability to see behind red thrombus, and the need for displacement of blood for clear visualization of the artery wall which requires a non-negligible amount of contrast medium; insufficient flushing may give the false impression of thrombus or dissection flap. Caution is required for possible artefacts (e.g. tangential drop-out mimicking plaque rupture) and for differentiation of calcific vs. lipid-rich plaque.

Near-infrared spectroscopy (currently not widely available) is based on the differential absorption of light by organic molecules and has shown good specificity (90%) but modest sensitivity (50%) for lipid pool detection in coronary atheroma.¹² Near-infrared spectroscopy is capable of identifying relatively superficial lipid cores (with a cap thickness $<450\ \mu\text{m}$). Angioscopy, a technique that allows for direct plaque visualization, is reviewed elsewhere.¹³

Limitations of IC imaging include the inability to pass catheters through severely stenotic, calcified, or tortuous lesions; the relatively high cost; and the need for trained operators for interpretation of findings. Although there are inherent risks related to the introduction of probes into the coronary arteries (e.g. dissection, thrombus formation) and to flushing (induction of ventricular fibrillation), these events remain infrequent and the methods are safe in the hands of experienced operators.¹⁴

In vivo assessment of vulnerable plaque and clinical implications

Approximately two-thirds of lethal coronary thrombosis is attributed to ruptured TCFAs.^{15,16} Accordingly, intact TCFAs are by inference considered vulnerable plaques at high risk to rupture and trigger acute coronary syndromes (ACS).¹⁵ In addition, superficial erosion is increasingly recognized as the underlying mechanism in a proportion of ACS.¹⁷ Because current modalities cannot differentiate features of plaques prone to undergo superficial erosion, and until we better understand the natural history of 'erosion-prone' lesions, interest continues to focus on the *in vivo* identification of rupture-prone TCFAs. Intracoronary imaging modalities can detect vulnerable plaques and predict subsequent clinical events to some extent; whether these properties translate into improved clinical outcomes is not yet established.

Intracoronary imaging for detection of presumed vulnerable plaque

While current IC imaging modalities can evaluate indices of vulnerable plaques *in vivo* fairly accurately, no single modality alone can simultaneously assess cap thickness, necrotic core size, and the

magnitude of inflammation, i.e. the combination of histological TCFA characteristics.^{15,16} While necrotic core by IVUS-VH correlates with human histology,⁸ characterization of TCFA phenotype has not been validated and is inferential (defined as necrotic core abutting the lumen) since critical cap thickness of ruptured autopsied plaques (<65 or <54 μm ¹⁶) is far below the resolution of IVUS ($\approx 200 \mu\text{m}$). Only OCT is capable of measuring cap thickness; however, cut-offs associated with rupture may differ from autopsy due to plaque shrinkage in pathology specimens.¹⁸ Validation of TCFA by OCT against histology has shown excellent sensitivity (100%) and specificity (97%) but limited positive predictive value (41%).¹⁹ Macrophage accumulations can be visualized by OCT as signal-intense punctuate regions with strong signal attenuation¹¹ (Figure 1E); quantification of macrophage accumulations within fibroatheroma caps has shown good correlation with human histology.²⁰ The specificity of detecting macrophages defined as 'bright spots' (not necessarily with shadowing) at any location in the artery wall is lower due to components seen elsewhere in the intima that also appear as bright spots in OCT (e.g. cellular fibrous tissue, calcium-fibrous tissue interfaces, micro-calcifications, cholesterol crystals).²¹ Optical coherence tomography can also detect microvessels (Figure 1F) which have been correlated with plaque progression and vulnerability.²² The ability of NIRS to identify fibroatheromas is modest and enhanced when combined with IVUS²³; NIRS can accurately detect lipid pools but cannot pinpoint TCFA in the absence of anatomical information. Moreover, IC imaging can capture features of rupture-prone lesions including

positive remodelling²⁴ and spotty calcification⁶ (IVUS); complex plaque morphology with evidence of previous rupture (IVUS), as well as plaque elasticity and deformability (IVUS palpography²⁵). Subclinical rupture is not infrequent in patients presenting with ACS or stable CAD²⁶; among ruptured lesions, IVUS and OCT correlates of clinical manifestation as an ACS include larger plaque burden, greater luminal narrowing, and more thrombus.²⁶

Intracoronary imaging for prediction of clinical events

The PROSPECT study using three-vessel IVUS in ACS patients showed that non-culprit lesions combining plaque burden $\geq 70\%$, minimal lumen area (MLA) $\leq 4 \text{ mm}^2$, and TCFA phenotype by IVUS-VH had an 11-fold higher risk of triggering subsequent major adverse cardiovascular events (MACE) compared with lesions without these characteristics.²⁷ Intravascular ultrasound-virtual histology TCFA phenotype alone was associated with a three-fold higher risk than non-TCFA lesions to result in MACE, most commonly rehospitalization due to angina with very infrequent hard endpoints.²⁷ Consistent findings were reported by the single-centre VIVA²⁸ and ATHEROREMO-IVUS studies.²⁹ It is notable that the identified lesion-specific characteristics did not correlate with classical angiographic and clinical risk predictors, indicating incremental prognostic benefit,³⁰ but also that they were highly prevalent ($\sim 40\text{--}50\%$ of patients) and had high negative, but low positive predictive value for MACE prediction (Figure 2). Based on the high

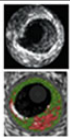
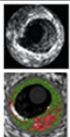
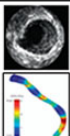

Study	Modality	Lesion characteristic(s)	Clinical endpoint	Positive predictive value	Negative predictive value
PROSPECT <i>n</i> =697	 IVUS & IVUS-VH	PB $\geq 70\%$ & MLA $< 4 \text{ mm}^2$ & IVUS-VH TCHA	MACE	18%	98%
ATHEROREMO IVUS <i>n</i> =581	 IVUS & IVUS-VH	PB $\geq 70\%$ & MLA $< 4 \text{ mm}^2$ & IVUS-VH TCHA	MACE	23%	93%
PREDICTION <i>n</i> =506	 IVUS & ESS	PB $\geq 58\%$ & Low ESS $< 1.0 \text{ Pa}$	PCI	41%	92%
ATHEROREMO NIRS <i>n</i> =203	 NIRS	LCBI _{4mm} > 43	MACE	12%	99%

Figure 2 Summary of the positive and negative predictive values of intracoronary imaging-derived variables for prediction of clinical outcomes in the PROSPECT,²⁷ ATHEROREMO-IVUS,²⁹ PREDICTION,³¹ and ATHEROREMO-NIRS³² studies. ESS, endothelial shear stress; LCBI, lipid-core burden index; MACE, major adverse cardiac events; MLA, minimal lumen area; PB, plaque burden; PCI, percutaneous coronary interventions.

accuracy to exclude, but limited potential to predict future events when using non-serial IC imaging, pre-emptive interventional treatment of presumed high-risk lesions cannot be supported at this stage. The PREDICTION study demonstrated the incremental value of low baseline shear stress to predict clinically relevant lesion progression requiring PCI.³¹ In ATHEROREMO-NIRS, a baseline value of lipid-core burden index (LCBI, the ratio of yellow pixels within the analysed segment divided by all viable pixels) above vs. below the median was associated with four-fold higher risk of MACE throughout 1 year, yet again with low positive predictive value.³² Prospective OCT studies investigating the predictive merit of minimal cap thickness and TCFA detection are currently not available.

In addition to asymptomatic, non-culprit lesions, detection of TCFA by IVUS-VH³³ or lipid-core plaques by NIRS³⁴ in lesions planned for PCI can identify patients at high risk for periprocedural complications [myocardial infarction (MI), distal embolization]. Preventive clinical strategies and dedicated embolic protection devices³⁵ have been proposed based on these imaging findings but have not yet entered routine clinical practice. Moreover, identification of plaque rupture vs. erosion by OCT as the triggering mechanism of ACS has been associated with worse clinical outcomes.³⁶ These results, however, require confirmation considering the atypically high reported event rates³⁶ as well as the inability of OCT (despite its high resolution) to detect endothelial denudation and absence of endothelial cells, i.e. defining characteristic of plaque erosion. *In vivo* evidence of erosion remains indirect, based on the presence of thrombus and absence of fibrous cap rupture¹⁷—an approach likely conducive to some imprecision.

Assessment of plaque progression/regression by intracoronary imaging

Evidence and determinants of plaque volume regression by intravascular ultrasound

Serial IVUS progression/regression studies are presented in Supplementary material online, *Tables S1* and *S2*. Among different measures of disease burden, change in per cent atheroma volume (PAV, i.e. percentage of vessel wall volume occupied by atheroma) is recommended due to smaller variability compared with other endpoints that may be sensitive to pullback length differences.⁵ In patients treated with statins or other medications with anti-atherosclerotic properties (ezetimibe; darapladip; reconstituted HDL; antihypertensive drugs; insulin-sensitizers in diabetic patients), IVUS studies have shown the absence of progression³⁷ and even modest regression with high-intensity statin therapy, documented as PAV reduction by -1% with atorvastatin 80 mg³⁸ and by -0.8 to -1.2% with rosuvastatin 40 mg.^{38–40} The finding of plaque progression in one-fifth of patients despite LDL-cholesterol (LDL-C) levels <70 mg/dL⁴¹ and in at least one-third of patients receiving high-intensity statin therapy^{38–40} likely reflects the multifactorial nature of the disease as well as limitations of currently available pharmacological treatments. Factors associated with

statin-mediated plaque regression include high baseline PAV, and lower on-treatment levels of LDL-C and C-reactive protein.⁴²

Clinical significance of plaque volume regression

Large global atheroma burden by IVUS has been identified as a predictor of subsequent clinical events.⁴³ The clinical significance of serial changes of PAV remains elusive. In a pooled analysis of six serial IVUS studies including >4000 patients, PAV progression was an independent predictor of MACE, a finding that was driven by repeat revascularizations (not clearly attributable to previously imaged segments) and not by MI or mortality.⁴⁴ Although high-intensity statin regimens can reverse the process of IVUS-defined anatomic plaque growth, a clear association of plaque regression with improved clinical outcomes has yet to be determined.

Intracoronary imaging to detect reversal of plaque vulnerability

While statins effectively reversed high-risk plaque characteristics in experimental and human histological studies,⁴⁵ IVUS-VH studies have shown stabilization, but no net reduction of necrotic core in response to statins^{40,46} or non-statin agents.²⁵ The absence of clinical benefit with one regimen (darapladip)⁴⁷ that was associated with stabilization of necrotic core (a secondary endpoint of the IBIS-2 study)²⁵ suggests that the use of IVUS-VH and other imaging-based endpoints as surrogates of clinical outcomes requires caution. In contrast, usual-dose atorvastatin resulted in fibrous cap thickening and reduction of macrophage accumulations as assessed by serial OCT⁴⁸—with the methodological caveat of manual cap thickness measurement. Similarly, maximal LCBI of obstructive lesions by NIRS decreased in response to high-dose rosuvastatin⁴⁹ (*Figure 3*).

Temporal evolution of vulnerable plaques by intracoronary imaging

The ability not only to detect a presumed vulnerable plaque at a single time-point but also to predict its subsequent biological behaviour is less well established, yet clinically highly relevant. The temporal evolution of plaque morphology by IVUS-VH has been assessed only in small patient cohorts and provided conflicting results. One study with predominantly stable CAD patients reported that 75% of IVUS-VH TCFA subsequently regressed to lower-risk phenotypes⁵⁰; factors associated with persistent IVUS-VH TCFA morphology included proximal localization, larger plaque burden and lesion length.⁵⁰ In contrast, other studies demonstrated temporal stability of IVUS-VH lesion morphology,⁵¹ even in the presence of high-intensity statin therapy.⁴⁰ In keeping with animal models associating local haemodynamic factors—in particular, low endothelial shear stress—with subsequent development of TCFA with highest risk characteristics,^{52,53} baseline shear stress has been associated in humans with greater subsequent plaque progression³¹ and necrotic core expansion by IVUS-VH.⁵⁴ Assessment of local haemodynamics holds substantial promise for prediction of vascular behaviour but is currently limited by the time-consuming and labour-intensive processes involved.

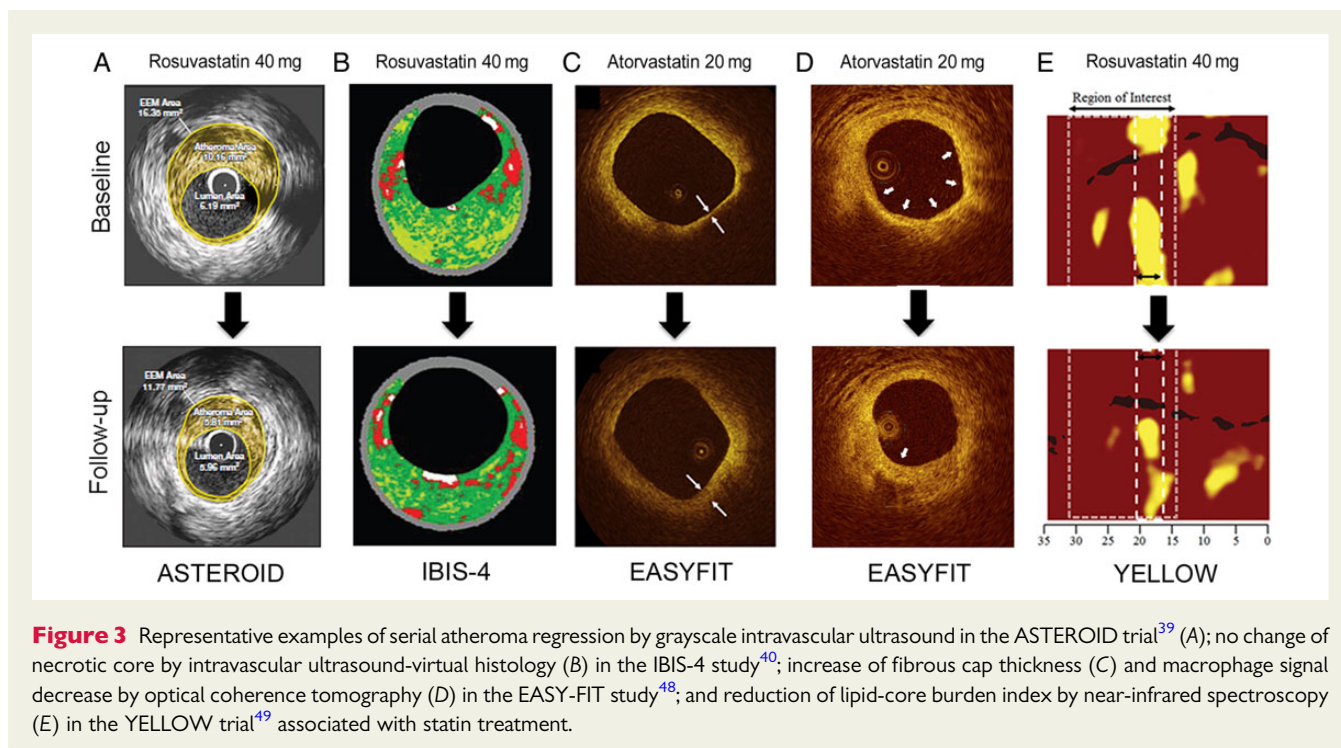


Figure 3 Representative examples of serial atheroma regression by grayscale intravascular ultrasound in the ASTEROID trial³⁹ (A); no change of necrotic core by intravascular ultrasound-virtual histology (B) in the IBIS-4 study⁴⁰; increase of fibrous cap thickness (C) and macrophage signal decrease by optical coherence tomography (D) in the EASY-FIT study⁴⁸; and reduction of lipid-core burden index by near-infrared spectroscopy (E) in the YELLOW trial⁴⁹ associated with statin treatment.

Intracoronary imaging for guiding coronary interventions

While IC imaging for characterization of asymptomatic, non-culprit lesions is currently a research tool with potential for clinical utility, IVUS and OCT are used increasingly to assess angiographically ambiguous lesions, guide and optimize PCI, and determine mechanisms of stent failure (Figure 4).

Intracoronary imaging to enhance decision-making in angiographically ambiguous lesions

In daily interventional practice, operators are frequently confronted with dilemmas when angiography alone is insufficient to establish the clinical significance of a given lesion. Although these scenarios are difficult to capture in scientific studies, IC imaging can be valuable for decision-making in clinically challenging, angiographically inconclusive cases. While there is no concrete evidence for direct comparisons, OCT is at least equally valuable and often superior to IVUS owing to its higher resolution^{55,56}; however, the inability of OCT probes to achieve sufficient flushing through severely stenotic vessels, to reach distal lesions, or to assess large-calibre segments (e.g. ostial left main lesions) also require consideration. Figure 5 shows representative examples from daily clinical practice, illustrating how IC imaging may affect the therapeutic strategy.

Intravascular ultrasound for assessment of intermediate non-left main lesions

Defining the haemodynamic relevance of angiographically intermediate lesions may be challenging. While an MLA ≥ 4 mm² signifies non-left main lesions where PCI may be safely deferred,⁵⁷ substantially different cut-offs have also been proposed.⁵⁸ Currently, haemodynamic

assessment with fractional flow reserve (FFR) or non-invasive ischaemia testing, and not morphometric assessment by IVUS or OCT,⁵⁹ is preferred for evaluation of intermediate non-left main lesions.⁶⁰

Intravascular ultrasound for evaluation of left main lesions

Angiographic assessment of left main disease may be hampered by the short length, absence of clear reference segment, and possible reverse tapering. Angiographic evaluation of intermediate left main lesions is associated with a high intra- and inter-observer variability, is frequently unreliable in ostial lesions,⁶¹ and cannot accurately define circumferential and longitudinal plaque distribution in distal and bifurcation lesions.⁶² The use of FFR is challenging in left main stenoses, as measurements may be falsely raised due to dampened catheter pressure (particularly in ostial lesions) or co-existing downstream disease (particularly in the LAD).⁶³ Currently, IVUS assumes class IIa indication to assess the severity of unprotected left main lesions.⁶⁰ An MLA of 7.5 cm² is the lower range for a normal left main stem.⁶⁴ Minimal lumen area < 5.9 mm² by IVUS correlated with FFR-defined ischaemia in one study,⁶⁵ although lower cut-offs (< 4.8 mm²) best predicted FFR < 0.80 among Asian patients—likely reflecting ethnicity-related differences.⁶⁶ Currently, an MLA > 6 mm² appears to be a safe cutoff for deferring PCI.⁶⁷ In distal left main and bifurcation lesions, IVUS can define longitudinal plaque distribution; IVUS pullbacks from both the LAD and LCX may be of additional value to plan the procedure.⁶⁸

Intravascular ultrasound for percutaneous coronary intervention guidance and optimization

Prior to stenting, IVUS can assess reference lumen dimension at the proximal and distal non-diseased reference sites, and also (unlike OCT) the external elastic membrane area at the site of minimal

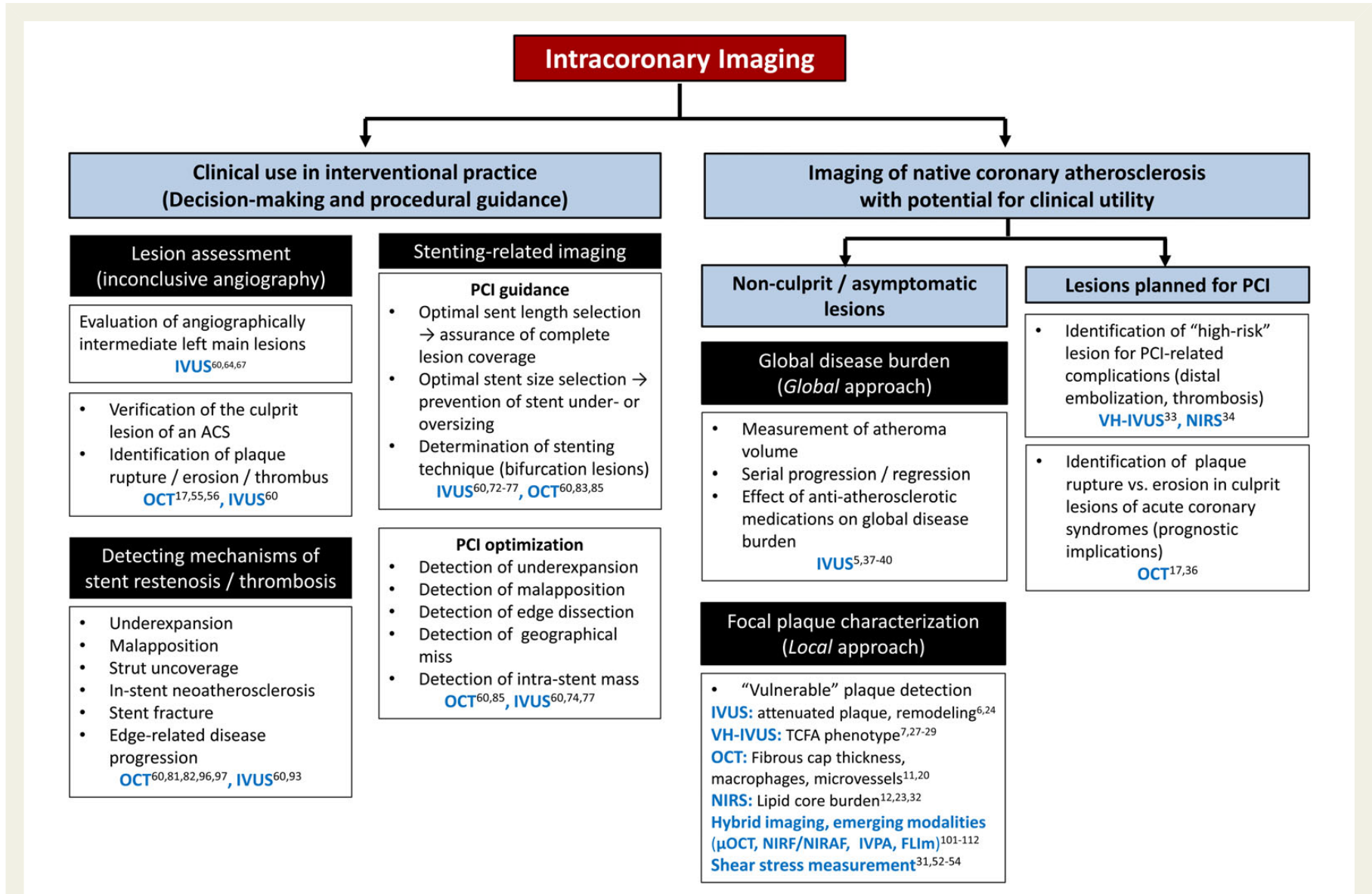


Figure 4 Schematic presentation of the current utility and potential implications of intracoronary imaging for guidance of coronary interventions and characterization of native atherosclerotic plaque.

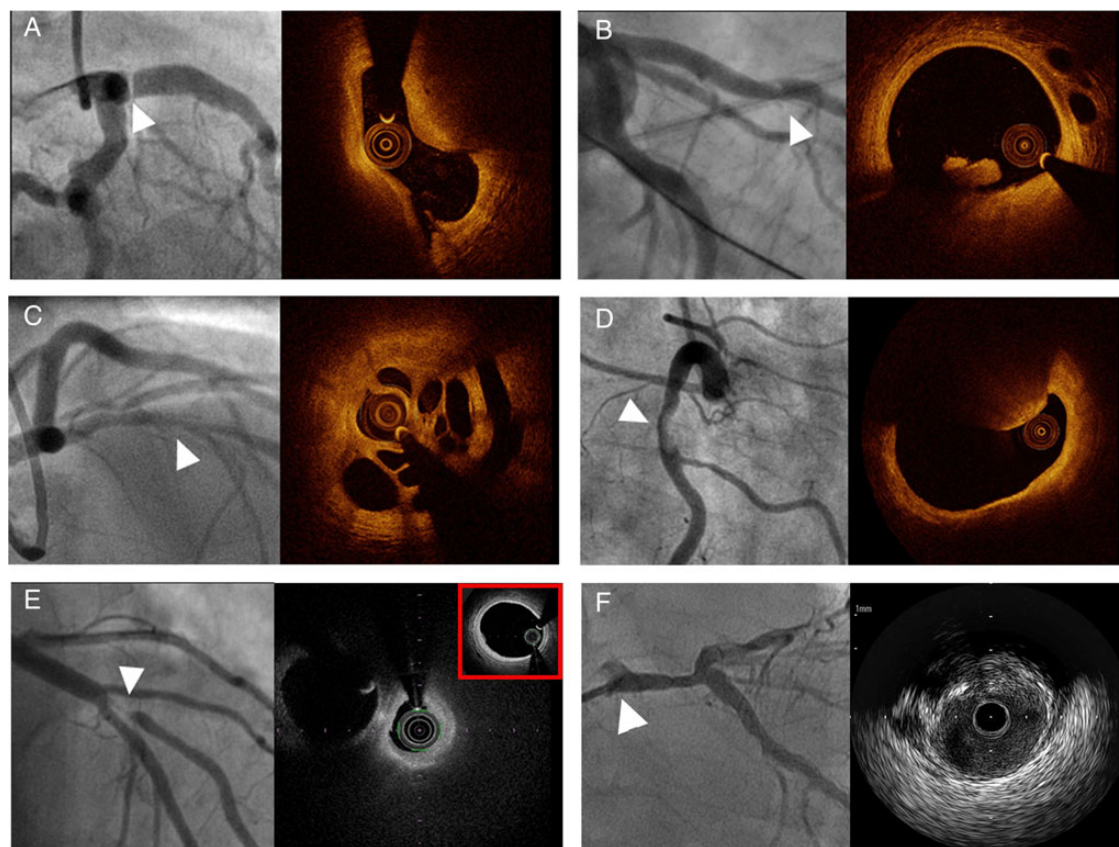


Figure 5 Unclear angiographic findings unravelled by intracoronary imaging. (A) Angiography shows a ‘fold’ at the ostium of the left anterior descending artery, only visible in one single angiographic projection, corresponding to an eccentric stenosis with significant lumen narrowing as evidenced by optical coherence tomography. (B) Discrete haziness in the mid-left anterior descending artery in a 30-year-old male with ventricular fibrillation and absence of ischemic ECG changes. Optical coherence tomography suggests the presence of erosion on top of a fibrous plaque, enabling the diagnosis of acute coronary syndromes-induced ventricular fibrillation. (C) Diffuse haziness in the mid-left anterior descending artery of a 31-year-old male. The multi-hole appearance in optical coherence tomography unravels recanalized thrombus. (D) Haziness in the right coronary artery suggestive of either thrombus or calcium. Optical coherence tomography shows evidence of calcification protruding in the lumen. (E) Subtotal stenosis of a diagonal branch in a 28-year-old female without coronary risk factors raised suspicion of spontaneous dissection or thrombo-embolic origin. Optical coherence tomography, however, indicates the presence of atherosclerosis with a normal mid-left anterior descending artery (red inset) and a severely stenotic thick-cap fibroatheroma in the diagonal branch. (F) Angiographic image of an intermediate ostial left main lesion (arrowhead, left) and corresponding intravascular ultrasound at the ostium, showing an eccentric plaque with minimal lumen area 4.8 cm^2 indicating relevant ostial stenosis.

lumen diameter. Information regarding lesion length, presence, and extent of calcification can optimize selection of stent size and stenting strategy. Following implantation, IVUS can detect correctable abnormalities related to the stent and underlying vessel wall which have been associated with the risk of restenosis or thrombosis including stent underexpansion,⁶⁹ malapposition, edge dissection, and geographic plaque miss. Although different criteria have been proposed, minimal stent area $<80\%$, the average proximal and distal reference lumen area is a comprehensive, widely applied cut-off for relevant underexpansion. Uniform, standardized criteria for PCI optimization in relation to IVUS findings remain to be established and currently represent a great unmet need.

In the era of bare-metal stents (BMS), IVUS guiding was associated with reduced restenosis and lower revascularization rates with no effect on mortality.⁷⁰ In the era of drug-eluting stents (DESs), some underpowered studies showed no clinical benefit of IVUS guidance

despite larger post-intervention stent dimensions,⁷¹ suggesting that the beneficial impact of IVUS guidance might be camouflaged by the overall improved efficacy of PCI with DES. Earlier randomized studies have not been able to demonstrate superiority of routine IVUS guidance compared with angiography-guided PCI regarding mortality, MACE, or stent thrombosis, likely because of small sample sizes and the inclusion of patients with predictably low benefit from IVUS guidance.^{71–73} Recently, however, the superiority of IVUS-guided vs. angiography-guided PCI was shown in the IVUS-XPL randomized trial including 1400 patients treated with DES for long ($\geq 28\text{mm}$) coronary lesions.⁷⁴ The study showed that the use of IVUS-guided everolimus-eluting stent implantation resulted in a significant reduction of MACE, a difference that was driven by a reduction in target lesion revascularization and not cardiac mortality or MI.⁷⁴ Along the same lines of the latter trial, observational studies (with inherent biases and limitations) reported consistent reductions

in ischemic outcomes,⁷⁵ and meta-analyses of mainly observational studies including >25 000 patients showed decrease in stent thrombosis, mortality, MI, and revascularization associated with IVUS-guided PCI.^{76,77} Overall, current evidence (built mainly on observational studies and one randomized trial⁷⁴) suggests greater benefit of IVUS- vs. angiography-guided PCI in complex lesions and ACS patients—although there are conflicting results regarding the latter.⁷⁸ The ongoing SYNTAX II trial (NCT02015832) investigates clinical outcomes of FFR- and IVUS-guided PCI in three-vessel disease using a newer-generation biodegradable polymer, everolimus-eluting stent.

Intravascular ultrasound-guided left main percutaneous coronary intervention

The clinical value of IVUS-guided PCI appears particularly evident in left main interventions. In a recent observational study of 1670 patients treated with DES, IVUS guidance was associated with reduced cardiac death, MI, revascularization, and stent thrombosis throughout 3 years.⁷⁹ The observational MAIN-COMPARE study showed a trend for lower mortality, but intriguingly no difference in MI or revascularization associated with IVUS guidance, thereby not providing mechanistic explanation for the observed mortality benefit.⁸⁰ Two randomized trials, EXCEL (NCT01205776) and NOBLE (NCT01496651), are currently underway comparing PCI vs. CABG in unprotected left main disease; IVUS guidance is recommended per protocol and important insights are expected.

Optical coherence tomography-guided percutaneous coronary intervention

Due to its high resolution, OCT is more accurate than IVUS for visualizing subtle stent- or lumen-related morphologies including edge and in-stent dissection, malapposition, residual thrombus, and tissue prolapse. While small post-intervention stent area and irregular protrusion have been associated with subsequent mid-term clinical outcomes,⁸¹ subtle abnormalities (malapposition with short strut-vessel distance, minor edge dissection) are likely not significant and possibly do not require correction⁸² but this warrants definitive evaluation. Similar to IVUS, standardized criteria for OCT-guided PCI optimization remain to be defined. Only one observational study has compared OCT- vs. angiography-guided PCI and reported reduced cardiac death and MACE in patients interrogated with OCT⁸³ on the background of relevant methodological limitations.⁸⁴ The non-randomized ILLUMIEN-I study reported that pre- and post-stenting OCT changed the procedural strategy in 57 and 27% of cases, respectively.⁸⁵ One small randomized study reported more underexpansion and greater residual reference segment stenosis with OCT- vs. IVUS-guided PCI.⁸⁶ The ongoing randomized OPINION trial (NCT01873027) directly compares IVUS vs. OCT guidance with respect to clinical outcomes following PCI with DES; preliminary results indicate comparable in-segment minimal lumen diameter after PCI, and 1-year clinical outcomes are expected soon (Prof. T. Akasaka, personal communication).

Intracoronary imaging to guide percutaneous coronary intervention with bioresorbable scaffolds

The role of IC imaging is particularly relevant with the use of bioresorbable scaffold (BRS). Meticulous attention to the implantation

technique appears to be more relevant compared with metallic DES, potentially related to greater strut thickness, reduced radial force, and less tolerance to post-dilatation.⁸⁷ The use of IC imaging may be a valuable adjunct for optimal scaffold size selection prior to implantation and to identify sub-optimal expansion and apposition or scaffold fracture after the implantation.⁸⁸ Observational studies confirmed that the use of imaging-assisted BRS implantation can provide similar post-procedural results compared with metallic DES.⁸⁹ While appropriately designed studies are required to establish the role of IC imaging for BRS implantation, we believe that routine use of IC imaging may be a reasonable strategy until further improvements of BRS devices with greater procedural flexibility and less rigorous performance standards become available.⁹⁰

Intravascular ultrasound and optical coherence tomography for determining the mechanism of stent failure

Intravascular ultrasound and OCT both assume class IIa indication to assess mechanical stent problems responsible for in-stent restenosis or stent thrombosis.⁶⁰ While restenosis rates have decreased substantially with new-generation DES, the investigation of mechanisms causing stent or scaffold thrombosis is a subject of growing interest. Intracoronary imaging studies consistently identified underexpansion and large dissections as correlates of early (acute/subacute) thrombosis,⁹¹ and malapposition and uncovered stent struts—which can be visualized with OCT⁹²—as mechanisms of late and very late thrombosis.^{93–96} Malapposition can either be persistent (i.e. implantation-related) or late acquired; a distinction is impossible without serial imaging. While the role of late acquired malapposition in triggering thrombotic events is not disputed, the impact of persistent malapposition remains controversial,⁹⁶ yet it is unlikely that a relevant role is limited to the acquired category only. Neointimal formation, i.e. atherosclerosis formation in the nascent neointima, has been documented *in vivo* using OCT and IVUS-VH^{93,97}; it correlates with native disease progression (thus suggesting similar pathophysiological mechanisms)⁹⁸ and has been identified as an important cause of very late stent thrombosis.⁹⁵ Further insights are expected from PRESTIGE (NCT01300507), the largest European stent thrombosis registry to date. With the increasing use of BRS, interest in the investigation of device failure is high as the scaffold resorption process *per se* may entail new pathomechanisms such as late scaffold disintegration in the presence of insufficient scaffold coverage by neointima.⁹⁹

New developments and future directions in intracoronary imaging

Combination of intravascular ultrasound/optical coherence tomography with near-infrared spectroscopy in a single catheter

Combined structural imaging with IVUS and plaque composition assessment with NIRS has been suggested to enhance coronary plaque characterization.¹⁰⁰ A hybrid IVUS–NIRS catheter is clinically

available and showed greater accuracy than IVUS or NIRS alone for the detection of plaques containing necrotic cores or large lipid pools.²³ A combined OCT-NIRS catheter with similar characteristics as current OCT technology has been proposed,¹⁰¹ and first human use of IC OCT-NIRS is expected in the near future.

Combination of optical coherence tomography and intravascular ultrasound in a single catheter

Intravascular ultrasound and OCT are, in many aspects, complementary for coronary plaque characterization (Table 1). The use of two separate catheters requires a time-consuming image co-registration process that may be subject to inaccuracies. A dual-modality OCT–IVUS catheter was introduced,¹⁰² combining high resolution for cap thickness measurement while preserving deep penetration for necrotic core and plaque volume measurement *ex vivo* in human coronary arteries and *in vivo* in animal models.¹⁰³ Remaining challenges for clinical use of the device include conformation of the imaging rate of IVUS to the higher speed of second-generation OCT, image fusion and display, and configuration of catheter size and mechanical properties for safe use in humans.

Advanced optical coherence tomography imaging technology

Novel approaches for polarization sensitive OCT (PS-OCT) catheters can provide measures of tissue birefringence and light depolarization in the context of microstructural morphological OCT images. In cadaver coronary arteries, PS-OCT assessed microstructural arrangement of fibrous cap collagen¹⁰⁴—a critical determinant of lesion stability.¹⁵ Studies validating PS-OCT are currently ongoing. In addition, spectroscopic OCT (SOCT) has been proposed for depth-resolved detection of lipid from OCT data.¹⁰⁵

One-micron resolution imaging

Our current understanding of human CAD has been limited by an inability to observe cellular and extracellular components *in vivo*. One-micron resolution OCT (μ OCT) uses a very broad bandwidth light source (i.e. 650–950 μ m), common path spectral-domain OCT and relatively large numerical aperture, yielding an axial and spatial resolution of 1 and 2 μ m, respectively.¹⁰⁶ In cadaver human coronary arteries, μ OCT enables clear visualization and quantification of *in situ* macrophages and cholesterol crystals (Figure 6A), as well as smooth muscle cells, platelet aggregation, and micro-calcifications.¹⁰⁶ The development of μ OCT for *in vivo* human use is currently ongoing, with an expectation of first-in-man use of a first-generation probe in the near future.

Combination of optical coherence tomography with near-infrared fluorescence in a single catheter

The use of exogenous agents (e.g. indocyanine green) allows standalone near-infrared fluorescence (NIRF) to detect plaque

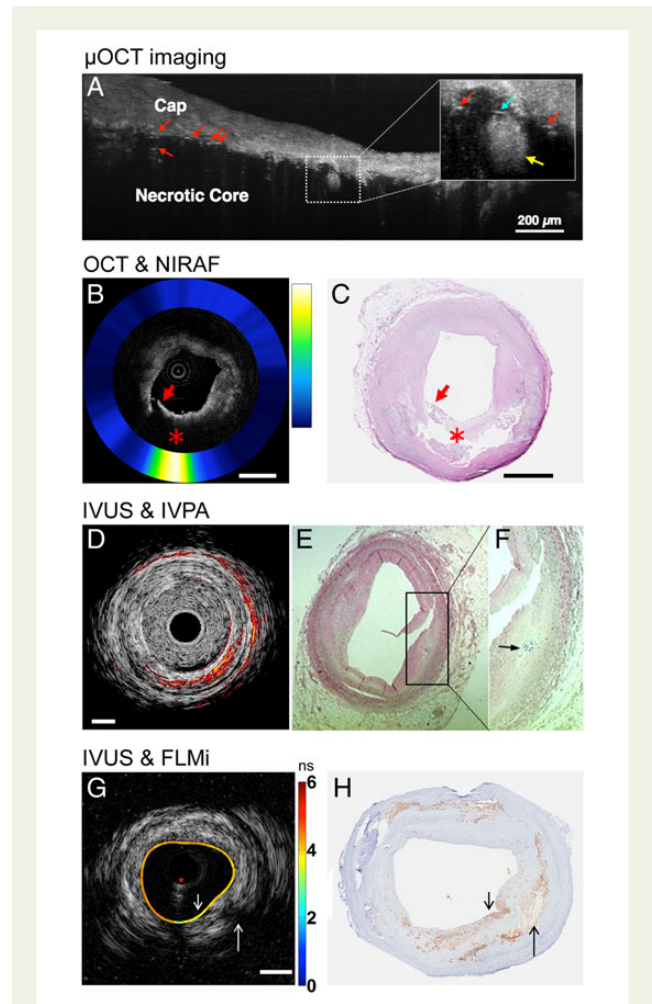


Figure 6 (A) One-micron optical coherence tomography image of a cadaver fibroatheromatous coronary plaque showing crystals in the necrotic core, seen as highly reflecting linear structures (red arrows). Inset ($\times 3$ magnification) demonstrates a macrophage (yellow arrow) phagocytosing a crystal (cyan arrow). (B) Dual-modality optical coherence tomography–near-infrared autofluorescence *ex vivo* imaging of a human coronary artery. Near-infrared autofluorescence is visualized as a ring around the grey-scale optical coherence tomography image, using a colour map from blue (low signal) to white (high near-infrared autofluorescence signal). An area of high optical coherence tomography signal attenuation (asterisk) suggests the presence of a fibroatheroma with rupture of the thin fibrous cap (red arrow), confirmed by the matching H&E stained slide showing co-localization of the elevated near-infrared autofluorescence signal with the necrotic core location (C). (D) Intravascular ultrasound/intravascular photoacoustics imaging of human coronary artery *ex vivo*. Elevated intravascular photoacoustic signal is observed from a lipid deposit at 3–6 o'clock position, corresponding to intimal lipid accumulation (E and F). (G) Co-registered intravascular ultrasound and multispectral autofluorescence lifetime imaging data of a thick-capped fibroatheroma and corresponding CD68-stained section (H). Lowering of fluorescence lifetime measurements is observed over the fibroatheroma cap rich in macrophages. Adapted with permission from Wang *et al.*¹¹⁰ (B and C); Wang *et al.*¹¹¹ (D–F); and Fatakdawala *et al.*¹¹² (G, H).

inflammation and enzymatic activity *in vivo*.¹⁰⁷ To overcome the lack of structural information, an all-optical system for dual-modality OCT and NIRF with the same size and characteristics as a clinical OCT catheter was recently used for *in vivo* imaging of coronary-sized vessels in animal models.¹⁰⁸ Targeted molecular imaging in human patients is expected to be feasible with NIRF in the near future. Near-infrared autofluorescence (NIRAF) is an endogenous signal that was elevated in human aortic and coronary cadaver plaques with necrotic cores.¹⁰⁹ A clinical OCT-NIRAF system has been developed and enabled the acquisition of OCT images synchronized with plaque autofluorescence *ex vivo* (Figure 6B and C).¹¹⁰

Combination of intravascular ultrasound with intravascular photoacoustics

Intravascular photoacoustics (IVPA) can assess light absorption properties of tissue, providing information about its chemical composition in a depth-resolved, cross-sectional image format. Recent *ex vivo* studies suggested the ability to determine plaque composition (e.g. lipid) and, through the use of exogenous contrast agents, inflammation (Figure 6D–F).¹¹¹ Further developments (e.g. increasing IVPA imaging speed) are required for this hybrid modality to be used clinically and exogenous agents (i.e. IVPA nanoparticles) for human use are currently under evaluation.

Combination of intravascular ultrasound with autofluorescence lifetime imaging in a single catheter

Multispectral autofluorescence lifetime imaging (FLIm) allows the assessment of compositional aspects of the artery wall (collagen, elastin, cholesterol) with a penetration depth of $\sim 200 \mu\text{m}$ (Figure 6G and H).¹¹² An IVUS–FLIm catheter was recently designed.¹¹² The strength of this technology to quantify multiple relevant plaque constituents makes it a promising technology for plaque imaging, although several issues need to be addressed for clinical use.

Conclusions and future perspectives in intracoronary imaging

Intracoronary imaging of native atherosclerosis can quantify *in vivo* the global burden of CAD and identify individual lesions with presumed high-risk morphology. However, the high prevalence of imaging-defined TCFA (with a usually uncomplicated long-term course) inevitably raises the question how vulnerable plaque detection can shift the paradigm to guiding patient management. Currently, more evidence is needed to assess whether the information obtained by existing as well as emerging IC imaging adds incrementally and cost-effectively to clinical and non-invasively derived variables for improvement of clinical outcomes. Because no single modality is likely to acquire the entire spectrum of processes that contribute to adverse coronary events, we believe that the greatest promise for attaining sufficient predictive ability to justify pre-emptive coronary interventions in asymptomatic lesions lies with

Table 2 Summary of clinical scenarios where the use of intracoronary imaging is more likely to be useful

Diagnostic evaluation
• Detection of stent-related mechanical problems ⁶⁰
• Assessment of mechanisms of stent failure ⁶⁰
• Unclear angiographic findings
• Left main stenoses ⁶⁰
• Complex bifurcation lesions

PCI guidance and optimization in selected patients ⁶⁰
• Unprotected left main lesions ⁶⁰
• High-risk acute coronary syndromes
• Insufficient angiographic image acquisition (e.g. obesity, extreme angulations etc.)
• Implantation of bioresorbable scaffolds

Indications are supported by current guidelines when applicable, or otherwise reflect the authors' views in the absence of sufficient evidence to support definitive recommendations.

the development of multimodality imaging technologies. In the next 3 years we expect the results of two studies [PROSPECT II (NCT02171065) and Lipid Rich Plaque (NCT02033694)] currently evaluating a strategy of prophylactic interventions in high-risk plaques. Within the same timeframe we foresee that in-depth morphologic plaque characterization using advanced and hybrid modalities (IVUS-OCT, OCT-NIRS, μOCT) will be feasible in human patients, and the clinical relevance of the expected imaging insights will be tested with regard to prognostication and possibly patient management.

Regarding interventional procedures, IVUS currently assumes class IIa and OCT a class IIb indication to optimize stent implantation in selected patients; real-life penetration ranges from 5 to 10% in Europe to $> 70\%$ in Japan.^{66,113} Previous randomized trials established the ability of IVUS to improve procedural results but failed to demonstrate significant improvement of clinical outcomes, whereas a recent landmark trial was able to show the superiority of IVUS- over angiography-guided PCI for reduction of one-year target-lesion revascularization.⁷⁴ Due to the ease of use and interpretation of stent-related findings, we believe that OCT is likely to be the favourable technique in future trials. Until recent favorable evidence⁷⁴ is corroborated by subsequent trials and likely integrated into official recommendations, IC imaging will be indicated to facilitate decision-making in patients with unclear angiographic findings, guide-selected interventions and optimize the final PCI result particularly with left main or complex bifurcation lesions, BRS implantation and possibly high-risk ACS patients (Table 2). Despite the increasing appreciation of the incremental value of IC imaging over angiography for PCI optimization, the Achilles heel of catheter-based imaging currently is that the relevance of imaging findings when left uncorrected is not always clearly defined; therefore, criteria for corrective measures remain in part subjective and are left to the discretion of the individual operator. Future studies need to focus on determining specific criteria (e.g. thresholds of malapposition distance or dissection length) with proven efficacy to improve procedural and longer-term clinical PCI outcomes.

Supplementary material

Supplementary material is available at *European Heart Journal* online.

Authors' contributions

L.R. and K.K. conceived and designed the research; K.K., G.U. and L.R. drafted the manuscript; S.W. and G.T. made critical revision of the manuscript for key intellectual content.

Acknowledgements

We thank Dr Stefan Stortecky, Bern University Hospital, Switzerland, for providing images for *Figure 5A* and Drs Takenori Domei and Shoichi Kuramitsu, Kokura Memorial Hospital, Japan, for providing the images for *Figure 5F*.

References

1. Finegold JA, Asaria P, Francis DP. Mortality from ischaemic heart disease by country, region, and age: statistics from World Health Organisation and United Nations. *Int J Cardiol* 2013;**168**:934–945.
2. Roelandt JR, Serruys PW, Bom N, Gussenhoven WG, Lancee CT, ten Hoff H. Intravascular real-time, two dimensional echocardiography. *Int J Card Imaging* 1989;**4**:63–67.
3. Tobis JM, Mallery JA, Gessert J, Griffith J, Mahon D, Bessen M, Moriuchi M, McLeay L, McRae M, Henry WL. Intravascular ultrasound cross-sectional arterial imaging before and after balloon angioplasty in vitro. *Circulation* 1989;**80**:873–882.
4. Gussenhoven EJ, Essed CE, Lancee CT, Mastik F, Frietman P, van Egmond FC, Reiber J, Bosch H, van Urk H, Roelandt J. Arterial wall characteristics determined by intravascular ultrasound imaging: an in vitro study. *J Am Coll Cardiol* 1989;**14**:947–952.
5. Mintz GS, Garcia-Garcia HM, Nicholls SJ, Weissman NJ, Bruining N, Crowe T, Tardif JC, Serruys PW. Clinical expert consensus document on standards for acquisition, measurement and reporting of intravascular ultrasound regression/progression studies. *EuroIntervention* 2011;**6**:1123–1130.
6. Pu J, Mintz GS, Biro S, Lee JB, Sum ST, Madden SP, Burke AP, Zhang P, He B, Goldstein JA, Stone GW, Muller JE, Virmani R, Maehara A. Insights into echo-attenuated plaques, echolucent plaques, and plaques with spotty calcification: novel findings from comparisons among intravascular ultrasound, near-infrared spectroscopy, and pathological histology in 2,294 human coronary artery segments. *J Am Coll Cardiol* 2014;**63**:2220–2233.
7. Garcia-Garcia HM, Mintz GS, Lerman A, Vince DG, Margolis MP, van Es GA, Morel MA, Nair A, Virmani R, Burke AP, Stone GW, Serruys PW. Tissue characterisation using intravascular radiofrequency data analysis: recommendations for acquisition, analysis, interpretation and reporting. *EuroIntervention* 2009;**5**:177–189.
8. Nasu K, Tsuchikane E, Katoh O, Vince DG, Virmani R, Surmely JF, Murata A, Takeda Y, Ito T, Ehara M, Matsubara T, Terashima M, Suzuki T. Accuracy of in vivo coronary plaque morphology assessment: a validation study of in vivo virtual histology compared with in vitro histopathology. *J Am Coll Cardiol* 2006;**47**:2405–2412.
9. Thim T, Hagensen MK, Wallace-Bradley D, Granada JF, Kaluza GL, Drouet L, Paaske WP, Bøtker HE, Falk E. Unreliable assessment of necrotic core by virtual histology intravascular ultrasound in porcine coronary artery disease. *Circ Cardiovasc Imaging* 2010;**3**:384–391.
10. Yabushita H, Bouma BE, Houser SL, Aretz HT, Jang IK, Schlerendorf KH, Kauffman CR, Shishkov M, Kang DH, Halpern EF, Tearney GJ. Characterization of human atherosclerosis by optical coherence tomography. *Circulation* 2002;**106**:1640–1645.
11. Tearney GJ, Regar E, Akasaka T, Adriaenssens T, Barlis P, Bezerra HG. Consensus standards for acquisition, measurement, and reporting of intravascular optical coherence tomography studies: a report from the International Working Group for Intravascular Optical Coherence Tomography Standardization and Validation. *J Am Coll Cardiol* 2012;**59**:1058–1072.
12. Gardner CM, Tan H, Hull EL, Lissauskas JB, Sum ST, Meese TM, Jiang C, Madden SP, Caplan JD, Burke AP, Virmani R, Goldstein J, Muller JE. Detection of lipid core coronary plaques in autopsy specimens with a novel catheter-based near-infrared spectroscopy system. *JACC Cardiovasc Imaging* 2008;**1**:638–648.
13. Ishibashi F, Aziz K, Abela GS, Waxman S. Update on coronary angiography: review of a 20 year experience and potential application for detection of vulnerable plaque. *J Interv Cardiol* 2006;**19**:17–25.
14. Taniwaki M, Radu MD, Garcia-Garcia HM, Heg D, Kelbæk H, Holmvang L, Moschovitis A, Noble S, Pedrazzini G, Saunamäki K, Dijkstra J, Landmesser U, Wenaweser P, Meier B, Stefanini GG, Roffi M, Lüscher TF, Windecker S, Räber L. Long-term safety and feasibility of three-vessel multimodality intravascular imaging in patients with ST-elevation myocardial infarction: the IBIS-4 substudy. *Int J Cardiovasc Imaging* 2015;**31**:915–926.
15. Libby P. Mechanisms of acute coronary syndromes and their implications for therapy. *N Engl J Med* 2013;**368**:2004–2013.
16. Narula J, Nakano M, Virmani R, Kolodgie FD, Petersen R, Newcomb R, Malik S, Fuster V, Finn AV. Histopathologic characteristics of atherosclerotic coronary disease and implications of the findings for the invasive and noninvasive detection of vulnerable plaques. *J Am Coll Cardiol* 2013;**61**:1041–1051.
17. Jia H, Abtahian F, Aguirre AD, Lee S, Chia S, Lowe H, Kato K, Yonetsu T, Vergallo R, Hu S, Tian J, Lee H, Park SJ, Jang YS, Raffel OC, Mizuno K, Uemura S, Itoh T, Kakuta T, Choi SY, Dauerman HL, Prasad A, Toma C, McNulty I, Zhang S, Yu B, Fuster V, Narula J, Virmani R, Jang IK. In vivo diagnosis of plaque erosion and calcified nodule in patients with acute coronary syndrome by intravascular optical coherence tomography. *J Am Coll Cardiol* 2013;**62**:1748–1758.
18. Yonetsu T, Kakuta T, Lee T, Takahashi K, Kawaguchi N, Yamamoto G, Koura K, Hishikari K, Iesaka Y, Fujiwara H, Isobe M. In vivo critical fibrous cap thickness for rupture-prone coronary plaques assessed by optical coherence tomography. *Eur Heart J* 2011;**32**:1251–1259.
19. Fujii K, Hao H, Shibuya M, Imanaka T, Fukunaga M, Miki K, Tamaru H, Sawada H, Naito Y, Ohyanagi M, Hirota S, Masuyama T. Accuracy of OCT, grayscale IVUS, and their combination for the diagnosis of coronary TCFA: an ex vivo validation study. *JACC Cardiovasc Imaging* 2015;**8**:451–460.
20. Tearney GJ, Yabushita H, Houser SL, Aretz HT, Jang IK, Schlerendorf KH, Kauffman CR, Shishkov M, Halpern EF, Bouma BE. Quantification of macrophage content in atherosclerotic plaques by optical coherence tomography. *Circulation* 2003;**107**:113–119.
21. Phipps JE, Vela D, Hoyt T, Halaney DL, Mancuso JJ, Buja LM, Asmis R, Milner TE, Feldman MD. Macrophages and intravascular OCT bright spots: a quantitative study. *JACC Cardiovasc Imaging* 2015;**8**:63–72.
22. Taruya A, Tanaka A, Nishiguchi T, Matsuo Y, Ozaki Y, Kashiwagi M, Shiono Y, Orii M, Yamano T, Ino Y, Hirata K, Kubo T, Akasaka T. Vasa vasorum restructuring in human atherosclerotic plaque vulnerability: a clinical optical coherence tomography study. *J Am Coll Cardiol* 2015;**65**:2469–2477.
23. Kang SJ, Mintz GS, Pu J, Sum ST, Madden SP, Burke AP, Xu K, Goldstein JA, Stone GW, Muller JE, Virmani R, Maehara A. Combined IVUS and NIRS detection of fibroatheromas: histopathological validation in human coronary arteries. *JACC Cardiovasc Imaging* 2015;**8**:184–194.
24. Schoenhagen P, Ziada KM, Kapadia SR, Crowe TD, Nissen SE, Tuzcu EM. Extent and direction of arterial remodeling in stable versus unstable coronary syndromes: an intravascular ultrasound study. *Circulation* 2000;**101**:598–603.
25. Serruys PW, Garcia-Garcia HM, Buszman P, Erne P, Verheye S, Aschermann M, Duckers H, Bleie O, Dudek D, Bøtker HE, von Birgelen C, D'Amico D, Hutchinson T, Zambanini A, Mastik F, van Es GA, van der Steen AF, Vince DG, Ganz P, Hamm CW, Wijns W, Zaleski A. Effects of the direct lipoprotein-associated phospholipase A(2) inhibitor darapladib on human coronary atherosclerotic plaque. *Circulation* 2008;**118**:1172–1182.
26. Tian J, Ren X, Vergallo R, Xing L, Yu H, Jia H, Soeda T, McNulty I, Hu S, Lee H, Yu B, Jang IK. Distinct morphological features of ruptured culprit plaque for acute coronary events compared to those with silent rupture and thin-cap fibroatheroma: a combined optical coherence tomography and intravascular ultrasound study. *J Am Coll Cardiol* 2014;**63**:2209–2216.
27. Stone GW, Maehara A, Lansky AJ, de Bruyne B, Cristea E, Mintz GS, Mehran R, McPherson J, Farhat N, Marso SP, Parise H, Templin B, White R, Zhang Z, Serruys PW. A prospective natural-history study of coronary atherosclerosis. *N Engl J Med* 2011;**364**:226–235.
28. Calvert PA, Obaid DR, O'Sullivan M, Shapiro LM, McNab D, Densem CG, Schofield PM, Braganza D, Clarke SC, Ray KK, West NE, Bennett MR. Association between IVUS findings and adverse outcomes in patients with coronary artery disease: the VIVA (VH-IVUS in Vulnerable Atherosclerosis) Study. *JACC Cardiovasc Imaging* 2011;**4**:894–901.
29. Cheng JM, Garcia-Garcia HM, de Boer SP, Kardys I, Heo JH, Akkerhuis KM, Oemrawsingh RM, van Domburg RT, Ligthart J, Witberg KT, Regar E, Serruys PW, van Geuns RJ, Boersma E. In vivo detection of high-risk coronary plaques by radiofrequency intravascular ultrasound and cardiovascular outcome: results of the ATHEROREMO-IVUS study. *Eur Heart J* 2014;**3**:639–647.
30. Bourantas CV, Garcia-Garcia HM, Farooq V, Maehara A, Xu K, Gènéreux P, Diletti R, Muramatsu T, Fahy M, Weisz G, Stone GW, Serruys PW. Clinical and angiographic characteristics of patients likely to have vulnerable plaques: analysis from the PROSPECT study. *JACC Cardiovasc Imaging* 2013;**6**:1263–1272.

31. Stone PH, Saito S, Takahashi S, Makita Y, Nakamura S, Kawasaki T, Takahashi A, Katsuki T, Nakamura S, Namiki A, Hirohata A, Matsumura T, Yamazaki S, Yokoi H, Tanaka S, Otsuji S, Yoshimachi F, Honye J, Harwood D, Reitman M, Coskun AU, Papafaklis MI, Feldman CL. Prediction of progression of coronary artery disease and clinical outcomes using vascular profiling of endothelial shear stress and arterial plaque characteristics: the PREDICTION Study. *Circulation* 2012;**126**:172–181.
32. Oemrawsingh RM, Cheng JM, García-García HM, van Geuns RJ, de Boer SP, Simsek C, Kardys I, Lenzen MJ, van Domburg RT, Regar E, Serruys PW, Akkerhuis KM, Boersma E. Near-infrared spectroscopy predicts cardiovascular outcome in patients with coronary artery disease. *J Am Coll Cardiol* 2014;**64**:2510–2518.
33. Claessen BE, Maehara A, Fahy M, Xu K, Stone GW, Mintz GS. Plaque composition by intravascular ultrasound and distal embolization after percutaneous coronary intervention. *JACC Cardiovasc Imaging* 2012;**5**(3 Suppl):S111–S118.
34. Goldstein JA, Maini B, Dixon SR, Brilakis ES, Grines CL, Rizik DG, Powers ER, Steinberg DH, Shunk KA, Weisz G, Moreno PR, Kini A, Sharma SK, Hendricks MJ, Sum ST, Madden SP, Muller JE, Stone GW, Kern MJ. Detection of lipid-core plaques by intracoronary near-infrared spectroscopy identifies high risk of periprocedural myocardial infarction. *Circ Cardiovasc Interv* 2011;**4**:429–437.
35. Brilakis ES, Abdel-Karim AR, Papayannis AC, Michael TT, Rangan BV, Johnson JL, Banerjee S. Embolic protection device utilization during stenting of native coronary artery lesions with large lipid core plaques as detected by near-infrared spectroscopy. *Catheter Cardiovasc Interv* 2012;**80**:1157–1162.
36. Niccoli G, Montone RA, Di Vito L, Gramaglia M, Refaat H, Scalone G, Leone AM, Trani C, Burzotta F, Porto I, Aurigemma C, Prati F, Crea F. Plaque rupture and intact fibrous cap assessed by optical coherence tomography portend different outcomes in patients with acute coronary syndrome. *Eur Heart J* 2015;**36**:1377–1384.
37. Nissen SE, Tuzcu EM, Schoenhagen P, Brown BG, Ganz P, Vogel RA, Crowe T, Howard G, Cooper CJ, Brodie B, Grines CL, DeMaria AN. Effect of intensive compared with moderate lipid-lowering therapy on progression of coronary atherosclerosis: a randomized controlled trial. *JAMA* 2004;**291**:1071–1080.
38. Nicholls SJ, Ballantyne CM, Barter PJ, Chapman MJ, Erbel RM, Libby P, Raichlen JS, Uno K, Borgman M, Wolski K, Nissen SE. Effect of two intensive statin regimens on progression of coronary disease. *N Engl J Med* 2011;**365**:2078–2087.
39. Nissen SE, Nicholls SJ, Sipahi I, Libby P, Raichlen JS, Ballantyne CM, Davignon J, Erbel R, Fruchart JC, Tardif JC, Schoenhagen P, Crowe T, Cain V, Wolski K, Goormastic M, Tuzcu EM. Effect of very high-intensity statin therapy on regression of coronary atherosclerosis: the ASTEROID trial. *JAMA* 2006;**295**:1556–1565.
40. Räber L, Taniwaki M, Zaugg S, Kelbæk H, Roffi M, Holmvang L, Noble S, Pedrazzini G, Moschovitis A, Lüscher TF, Matter CM, Serruys PW, Jüni P, García-García HM, Windecker S. Effect of high-intensity statin therapy on atherosclerosis in non-infarct-related coronary arteries (IBIS-4): a serial intravascular ultrasonography study. *Eur Heart J* 2015;**36**:490–500.
41. Bayturan O, Kapadia S, Nicholls SJ, Tuzcu EM, Shao M, Uno K, Shreevatsa A, Lavoie AJ, Wolski K, Schoenhagen P, Nissen SE. Clinical predictors of plaque progression despite very low levels of low-density lipoprotein cholesterol. *J Am Coll Cardiol* 2010;**55**:2736–2742.
42. Puri R, Nissen SE, Ballantyne CM, Barter PJ, Chapman MJ, Erbel R, Libby P, Raichlen JS, St John J, Wolski K, Uno K, Kataoka Y, Nicholls SJ. Factors underlying regression of coronary atheroma with potent statin therapy. *Eur Heart J* 2013;**34**:1818–1825.
43. Puri R, Nissen SE, Shao M, Ballantyne CM, Barter PJ, Chapman MJ, Erbel R, Libby P, Raichlen JS, Uno K, Kataoka Y, Nicholls SJ. Coronary atheroma volume and cardiovascular events during maximally intensive statin therapy. *Eur Heart J* 2013;**34**:3182–3190.
44. Nicholls SJ, Hsu A, Wolski K, Hu B, Bayturan O, Lavoie A, Uno K, Tuzcu EM, Nissen SE. Intravascular ultrasound-derived measures of coronary atherosclerotic plaque burden and clinical outcome. *J Am Coll Cardiol* 2010;**55**:2399–2407.
45. Puato M, Faggini E, Rattazzi M, Zambon A, Cipollone F, Grego F, Ganassin L, Plebani M, Mezzetti A, Pauletto P. Atorvastatin reduces macrophage accumulation in atherosclerotic plaques: a comparison of a nonstatin-based regimen in patients undergoing carotid endarterectomy. *Stroke* 2010;**41**:1163–1168.
46. Puri R, Libby P, Nissen SE, Wolski K, Ballantyne CM, Barter PJ, Chapman MJ, Erbel R, Raichlen JS, Uno K, Kataoka Y, Tuzcu EM, Nicholls SJ. Long-term effects of maximally intensive statin therapy on changes in coronary atheroma composition: insights from SATURN. *Eur Heart J Cardiovasc Imaging* 2014;**15**:380–388.
47. O'Donoghue ML, Braunwald E, White HD, Lukas MA, Tarka E, Steg PG, Hochman JS, Bode C, Maggioni AP, Im K, Shannon JB, Davies RY, Murphy SA, Crugnale SE, Wiviott SD, Bonaca MP, Watson DF, Weaver WD, Serruys PW, Cannon CP. Effect of darapladib on major coronary events after an acute coronary syndrome: the SOLID-TIMI 52 randomized clinical trial. *JAMA* 2014;**312**:1006–1015.
48. Komukai K, Kubo T, Kitabata H, Matsuo Y, Ozaki Y, Takarada S, Okumoto Y, Shiono Y, Orii M, Shimamura K, Ueno S, Yamano T, Tanimoto T, Ino Y, Yamaguchi T, Kumiko H, Tanaka A, Imanishi T, Akagi H, Akasaka T. Effect of atorvastatin therapy on fibrous cap thickness in coronary atherosclerotic plaque as assessed by optical coherence tomography: the EASY-FIT study. *J Am Coll Cardiol* 2014;**64**:2207–2217.
49. Kini AS, Baber U, Kovacic JC, Limaye A, Ali ZA, Sweeny J, Maehara A, Mehran R, Dangas G, Mintz GS, Fuster V, Narula J, Sharma SK, Moreno PR. Changes in plaque lipid content after short-term intensive versus standard statin therapy: the YELLOW trial (reduction in yellow plaque by aggressive lipid-lowering therapy). *J Am Coll Cardiol* 2013;**62**:21–29.
50. Kubo T, Maehara A, Mintz GS, Doi H, Tsujita K, Choi SY, Katoh O, Nasu K, Koenig A, Pieper M, Rogers JH, Wijns W, Böse D, Margolis MP, Moses JW, Stone GW, Leon MB. The dynamic nature of coronary artery lesion morphology assessed by serial virtual histology intravascular ultrasound tissue characterization. *J Am Coll Cardiol* 2010;**55**:1590–1597.
51. Zhao Z, Witzentichler B, Mintz GS, Jaster M, Choi SY, Wu X, He Y, Margolis MP, Dressler O, Cristea E, Parise H, Mehran R, Stone GW, Maehara A. Dynamic nature of nonculprit coronary artery lesion morphology in STEMI: a serial IVUS analysis from the HORIZONS-AMI trial. *JACC Cardiovasc Imaging* 2013;**6**:86–95.
52. Koskinas KC, Sukhova GK, Baker AB, Papafaklis MI, Chantzis YS, Coskun AU, Quillard T, Jonas M, Maynard C, Antoniadis AP, Shi GP, Libby P, Edelman ER, Feldman CL, Stone PH. Thin-capped atheromata with reduced collagen content in pigs develop in coronary arterial regions exposed to persistently low endothelial shear stress. *Arterioscler Thromb Vasc Biol* 2013;**33**:1494–1504.
53. Koskinas KC, Feldman CL, Chantzis YS, Coskun AU, Jonas M, Maynard C, Baker AB, Papafaklis MI, Edelman ER, Stone PH. Natural history of experimental coronary atherosclerosis and vascular remodeling in relation to endothelial shear stress: a serial, in vivo intravascular ultrasound study. *Circulation* 2010;**121**:2092–2101.
54. Samady H, Eshtehardi P, McDaniel MC, Suo J, Dhawan SS, Maynard C, Timmins LH, Quyyumi AA, Giddens DP. Coronary artery wall shear stress is associated with progression and transformation of atherosclerotic plaque and arterial remodeling in patients with coronary artery disease. *Circulation* 2011;**124**:779–788.
55. Kubo T, Imanishi T, Takarada S, Kuroi A, Ueno S, Yamano T, Tanimoto T, Matsuo Y, Masho T, Kitabata H, Tsuda K, Tomobuchi Y, Akasaka T. Assessment of culprit lesion morphology in acute myocardial infarction: ability of optical coherence tomography compared with intravascular ultrasound and coronary angiography. *J Am Coll Cardiol* 2007;**50**:933–939.
56. Jang IK, Bouma BE, Kang DH, Park SJ, Park SW, Seung KB, Choi KB, Shikhov M, Schlenker D, Pomerantsev E, Houser SL, Arw HT, Tearney GJ. Visualization of coronary atherosclerotic plaques in patients using optical coherence tomography: comparison with intravascular ultrasound. *J Am Coll Cardiol* 2002;**39**:604–609.
57. Briguori C, Anzuini A, Airolidi F, Gemelli G, Nishida T, Adamian M, Corvaja N, Di Mario C, Colombo A. Intravascular ultrasound criteria for the assessment of the functional significance of intermediate coronary artery stenoses and comparison with fractional flow reserve. *Am J Cardiol* 2001;**87**:136–141.
58. Ben-Dor I, Torguson R, Gaglia MA Jr, Gonzalez MA, Maluenda G, Bui AB, Xue Z, Satler LF, Suddath WO, Lindsay J, Pichard AD, Waksman R. Correlation between fractional flow reserve and intravascular ultrasound lumen area in intermediate coronary artery stenosis. *EuroIntervention* 2011;**7**:225–233.
59. Gonzalo N, Escaned J, Alfonso F, Nolte C, Rodriguez V, Jimenez-Quevedo P, Bañuelos C, Fernández-Ortiz A, García E, Hernandez-Antolin R, Macaya C. Morphometric assessment of coronary stenosis relevance with optical coherence tomography: a comparison with fractional flow reserve and intravascular ultrasound. *J Am Coll Cardiol* 2012;**59**:1080–1089.
60. Windecker S, Kolh P, Alfonso F, Collet JP, Cremer J, Falk V, Filippatos G, Hamm C, Head SJ, Jüni P, Kappetein AP, Kastrati A, Knuuti J, Landmesser U, Laufer G, Neumann FJ, Richter DJ, Schauerte P, Sousa Uva M, Stefanini GG, Taggart DP, Torracca L, Valgimigli M, Wijns W, Witkowski A. 2014 ESC/EACTS Guidelines on myocardial revascularization: The Task Force on Myocardial Revascularization of the European Society of Cardiology (ESC) and the European Association for Cardio-Thoracic Surgery (EACTS). *Eur Heart J* 2014;**35**:2541–2619.
61. Sano K, Mintz GS, Carlier SG, de Ribamar Costa J Jr, Qian J, Missel E, Shan S, Franklin-Bond T, Boland P, Weisz G, Mousa I, Dangas GD, Mehran R, Lansky AJ, Kreps EM, Collins MB, Stone GW, Leon MB, Moses JW. Assessing intermediate left main coronary lesions using intravascular ultrasound. *Am Heart J* 2007;**154**:983–988.
62. Oviedo C, Maehara A, Mintz GS, Araki H, Choi SY, Tsujita K, Kubo T, Doi H, Templin B, Lansky AJ, Dangas G, Leon MB, Mehran R, Tahk SJ, Stone GW, Ochiai M, Moses JW. Intravascular ultrasound classification of plaque distribution in left main coronary artery bifurcations: where is the plaque really located? *Circ Cardiovasc Interv* 2010;**3**:105–112.

63. Daniels DV, van't Veer M, Pijls NHJ. The impact of downstream coronary stenoses on fractional flow reserve assessment of intermediate left main disease. *J Am Coll Cardiol Interv* 2012;**5**:1021–1025.
64. Fassa AA, Wagatsuma K, Higano ST. Intravascular ultrasound-guided treatment for angiographically indeterminate left main coronary artery disease: a long-term follow-up study. *J Am Coll Cardiol* 2005;**45**:204–211.
65. Jasti V, Ivan E, Yalamanchili V, Wongpraparut N, Leeser MA. Correlations between fractional flow reserve and intravascular ultrasound in patients with an ambiguous left main coronary artery stenosis. *Circulation* 2004;**110**:2831–2836.
66. Park SJ, Ahn JM, Kang SJ, Yoon SH, Koo BK, Lee JY, Kim WJ, Park DW, Lee SW, Kim YH, Lee CW, Park SW. Intravascular ultrasound-derived minimal lumen area criteria for functionally significant left main coronary artery stenosis. *JACC Cardiovasc Interv* 2014;**7**:868–874.
67. de la Torre Hernandez JM, Hernández Hernandez F, Alfonso F, Alfonso F, Rumoroso JR, Lopez-Palop R, Sadaba M, Carrillo P, Rondan J, Lozano I, Ruiz Nodar JM, Baz JA, Fernandez Nofrerias E, Pajin F, Garcia Camarero T, Gutierrez H. Prospective application of Pre-defined intravascular ultrasound criteria for assessment of intermediate left main coronary artery lesions results from the multicenter LITRO study. *J Am Coll Cardiol* 2011;**58**:351–358.
68. Oviedo C, Maehara A, Mintz GS, Tsujita K, Kubo T, Doi H, Castellanos C, Lansky AJ, Mehran R, Dangas G, Leon MB, Stone GW, Templin B, Araki H, Ochiai M, Moses JW. Is accurate intravascular ultrasound evaluation of the left circumflex ostium from a left anterior descending to left main pullback possible? *Am J Cardiol* 2010;**105**:948–954.
69. Liu X, Doi H, Maehara A, Mintz GS, Costa Jde R Jr, Sano K, Weisz G, Dangas GD, Lansky AJ, Kreps EM, Collins M, Fahy M, Stone GW, Moses JW, Leon MB, Mehran R. A volumetric intravascular ultrasound comparison of early drug-eluting stent thrombosis versus restenosis. *JACC Cardiovasc Interv* 2009;**2**:428–434.
70. Parise H, Maehara A, Stone GW, Leon MB, Mintz GS. Meta-analysis of randomized studies comparing intravascular ultrasound versus angiographic guidance of percutaneous coronary intervention in pre-drug-eluting stent era. *Am J Cardiol* 2011;**107**:374–382.
71. Jakabcin J, Spacek R, Bystron M, Kvasnák M, Jager J, Veselka J. Long-term health outcome and mortality evaluation after invasive coronary treatment using drug eluting stents with or without the IVUS guidance. Randomized control trial. HOME DES IVUS. *Catheter Cardiovasc Interv* 2010;**75**:578–583.
72. Chieffo A, Latib A, Caussin C, Presbitero P, Galli S, Menozzi A, Varbella F, Mauri F, Valgimigli M, Arampatzis C, Sabate M, Erglis A, Reimers B, Airolidi F, Laine M, Palop RL, Mikhail G, McCarthy P, Romeo F, Colombo A. A prospective, randomized trial of intravascular-ultrasound guided compared to angiography guided stent implantation in complex coronary lesions: the AVIO trial. *Am Heart J* 2013;**165**:65–72.
73. Kim JS, Kang TS, Mintz GS, Park BE, Shin DH, Kim BK, Ko YG, Choi D, Jang Y, Hong MK. Randomized comparison of clinical outcomes between intravascular ultrasound and angiography-guided drug-eluting stent implantation for long coronary artery stenoses. *J Am Coll Cardiol Interv* 2013;**6**:369–376.
74. Hong SJ, Kim BK, Shin DH, Nam CM, Kim JS, Ko YG, Choi D, Kang TS, Kang WC, Her AY, Kim Y, Hur SH, Hong BK, Kwon H, Jang Y, Hong MK. Effect of Intravascular Ultrasound-Guided vs Angiography-Guided Everolimus-Eluting Stent Implantation: The IVUS-XPL Randomized Clinical Trial. *JAMA* 2015; In Press.
75. Witzencbichler B, Maehara A, Weisz G, Neumann FJ, Rinaldi MJ, Metzger C, Henry TD, Cox DA, Duffy PL, Brodie BR, Stuckey TD, Mazzaferri EL, Xu K, Parise H, Mehran R, Mintz GS, Stone GW. Relationship between intravascular ultrasound guidance and clinical outcomes after drug-eluting stents: The Assessment of Dual Antiplatelet Therapy With Drug-Eluting Stents (ADAPT-DES) study. *Circulation* 2014;**129**:463–470.
76. Ahn JM, Kang SJ, Yoon SH, Park HW, Kang SM, Lee JY, Lee SW, Kim YH, Lee CW, Park SW, Mintz GS, Park SJ. Meta-analysis of outcomes after intravascular ultrasound-guided versus angiography-guided drug-eluting stent implantation in 26,503 patients enrolled in three randomized trials and 14 observational studies. *Am J Cardiol* 2014;**113**:1338–1347.
77. Jang JS, Song YJ, Kang W, Jin HY, Seo JS, Yang TH, Kim DK, Cho KI, Kim BH, Park YH, Je HG, Kim DS. Intravascular ultrasound-guided implantation of drug-eluting stents to improve outcome: a meta-analysis. *JACC Cardiovasc Interv* 2014;**7**:233–243.
78. Ahmed K, Jeong MH, Chakraborty R, Ahn Y, Sim DS, Park K, Hong YJ, Kim JH, Cho KH, Kim MC, Hachinohe D, Hwang SH, Lee MG, Cho MC, Kim CJ, Kim YJ, Park JC, Kang JC. Role of intravascular ultrasound in patients with acute myocardial infarction undergoing percutaneous coronary intervention. *Am J Cardiol* 2011;**108**:8–14.
79. de la Torre Hernandez JM, Baz Alonso JA, Gómez Hospital JA, Alfonso Manterola F, Garcia Camarero T, Gimeno de Carlos F, Roura Ferrer G, Recalde AS, Martínez-Luengas IL, Gomez Lara J, Hernandez Hernandez F, Pérez-Vizcayno MJ, Cequier Fillat A, Perez de Prado A, Gonzalez-Trevilla AA, Jimenez Navarro MF, Mauri Ferrer J, Fernandez Diaz JA, Pinar Bermudez E, Zueco Gil J. Clinical impact of intravascular ultrasound guidance in drug-eluting stent implantation for unprotected left main coronary disease: pooled analysis at the patient-level of 4 registries. *JACC Cardiovasc Interv* 2014;**7**:244–254.
80. Park SJ, Kim YH, Park DW, Lee SW, Kim WJ, Suh J, Yun SC, Lee CW, Hong MK, Lee JH, Park SW. Impact of intravascular ultrasound guidance on long-term mortality in stenting for unprotected left main coronary artery stenosis. *Circ Cardiovasc Interv* 2009;**2**:167–177.
81. Soeda T, Uemura S, Park SJ, Jang Y, Lee S, Cho JM, Kim SJ, Vergallo R, Minami Y, Ong DS, Gao L, Lee H, Zhang S, Yu B, Saito Y, Jang IK. Incidence and clinical significance of post-stent OCT findings: one year follow-up study from a multicenter registry. *Circulation* 2015; in press.
82. Kawamori H, Shite J, Shinke T, Otake H, Matsumoto D, Nakagawa M, Nagoshi R, Kozuki A, Hariki H, Inoue T, Osue T, Taniguchi Y, Nishio R, Hiranuma N, Hirata K. Natural consequence of post-intervention stent malapposition, thrombus, tissue prolapse, and dissection assessed by optical coherence tomography at mid-term follow-up. *Eur Heart J Cardiovasc Imaging* 2013;**14**:865–875.
83. Prati F, Di Vito L, Biondi-Zoccai G, Occhipinti M, La Manna A, Tamburino C, Burzotta F, Trani C, Porto I, Ramazzotti V, Imola F, Manzoli A, Materia L, Cremonesi A, Albertucci M. Angiography alone versus angiography plus optical coherence tomography to guide decision-making during percutaneous coronary intervention: the Centro per la Lotta contro l'Infarto-Optimisation of Percutaneous Coronary Intervention (CLI-OPCI) study. *EuroIntervention* 2012;**8**: 823–829.
84. Räber L, Radu MD. Optimising cardiovascular outcomes using optical coherence tomography-guided percutaneous coronary interventions. *EuroIntervention* 2012;**8**:765–771.
85. Wijns W, Shite J, Jones MR, Lee SW, Price MJ, Fabbicchi F, Barbato E, Akasaka T, Bezerra H, Holmes D. Optical coherence tomography imaging during percutaneous coronary intervention impacts physician decision-making: ILUMIEN I study. *Eur Heart J* 2015; in press.
86. Habara M, Nasu K, Terashima M, Kaneda H, Yokota D, Ko E, Ito T, Kurita T, Tanaka N, Kimura M, Ito T, Kinoshita Y, Tsuchikane E, Asakura K, Asakura Y, Katoh O, Suzuki T. Impact of frequency-domain optical coherence tomography guidance for optimal coronary stent implantation in comparison with intravascular ultrasound guidance. *Circ Cardiovasc Interv* 2012;**5**:193–201.
87. Serruys PW, Chevalier B, Dudek D, Cequier A, Carrié D, Iniguez A, Dominici M, van der Schaaf RJ, Haude M, Wasungu L, Veldhof S, Peng L, Staehr P, Grundeken MJ, Ishibashi Y, Garcia-Garcia HM, Onuma Y. A bioresorbable everolimus-eluting scaffold versus a metallic everolimus-eluting stent for ischaemic heart disease caused by de-novo native coronary artery lesions (ABSORB II): an interim 1-year analysis of clinical and procedural secondary outcomes from a randomised controlled trial. *Lancet* 2015;**385**:43–54.
88. Brown AJ, McCormick LM, Braganza DM, Bennett MR, Hoole SP, West NE. Expansion and malapposition characteristics after bioresorbable vascular scaffold implantation. *Catheter Cardiovasc Interv* 2014;**84**:37–45.
89. Mattesini A, Secco GG, Dall'Ara G, Ghione N, Rama-Merchan JC, Lupi A, Viceconte N, Lindsay AC, De Silva R, Foin N, Naganuma T, Valente S, Colombo A, Di Mario C. ABSORB biodegradable stents versus second-generation metal stents: a comparison study of 100 complex lesions treated under OCT guidance. *JACC Cardiovasc Interv* 2014;**7**:741–750.
90. Windecker S, Koskinas KC, Siontis GC. Bioresorbable scaffolds vs. metallic drug-eluting stents: are we getting any closer to a paradigm shift? *J Am Coll Cardiol* 2015; in press.
91. Parodi G, La Manna A, Di Vito L, Valgimigli M, Fineschi M, Bellandi B, Niccoli G, Giusti B, Valenti R, Cremonesi A, Biondi-Zoccai G, Prati F. Stent-related defects in patients presenting with stent thrombosis: differences at optical coherence tomography between subacute and late/very late thrombosis in the Mechanism Of Stent Thrombosis (MOST) study. *EuroIntervention* 2013;**9**:936–944.
92. Ughi GJ, Van Dyck CJ, Adriaenssens T, Hoymans VY, Sinnaeve P, Timmermans JP, Desmet W, Vrints CJ, D'Hooge J. Automatic assessment of stent neointimal coverage by intravascular optical coherence tomography. *Eur Heart J Cardiovasc Imaging* 2014;**15**:195–200.
93. Guagliumi G, Sirbu V, Musumeci G, Gerber R, Biondi-Zoccai G, Ikejima H, Ladich E, Lortkipanidze N, Matiashvili A, Valsecchi O, Virmani R, Stone GW. Examination of the in vivo mechanisms of late drug-eluting stent thrombosis: findings from optical coherence tomography and intravascular ultrasound imaging. *JACC Cardiovasc Interv* 2012;**5**:12–20.
94. Kang SJ, Lee CW, Song H, Ahn JM, Kim WJ, Lee JY, Park DW, Lee SW, Kim YH, Mintz GS, Park SW, Park SJ. OCT analysis in patients with very late stent thrombosis. *JACC Cardiovasc Imaging* 2013;**6**:695–703.
95. Souteyrand G, Amabile N, Mangin L, Cayla G, Finet G, Meneveau N, Range G, Barnay P, Trouillet C, Motreff P. Mechanisms of stent thrombosis analysed by optical coherence tomography: insights from the national PESTO French registry. In: Presented at the EuroPCR 2015 Conference.

96. Attizzani GF, Capodanno D, Ohno Y, Tamburino C. Mechanisms, pathophysiology, and clinical aspects of incomplete stent apposition. *J Am Coll Cardiol* 2014;**63**:1355–1367.
97. Kang SJ, Mintz GS, Akasaka T, Park DW, Lee JY, Kim WJ, Lee SW, Kim YH, Whan Lee C, Park SW, Park SJ. Optical coherence tomographic analysis of in-stent neoatherosclerosis after drug-eluting stent implantation. *Circulation* 2011;**123**:2954–2963.
98. Taniwaki M, Windecker S, Zaugg S, Stefanini GG, Baumgartner S, Zanchin T, Wenaweser P, Meier B, Juni P, Räber L. The association between in-stent neoatherosclerosis and native coronary artery disease progression: a long-term angiographic and optical coherence tomography cohort study. *Eur Heart J* 2015; in press.
99. Räber L, Brugaletta S, Yamaji K, O'Sullivan CJ, Otsuki S, Koppa T, Taniwaki M, Onuma Y, Freixa Y, Eberli F, Serruys P, Joner M, Sabaté M. Very late scaffold thrombosis: intracoronary imaging, histopathological and spectroscopy findings. *J Am Coll Cardiol* 2015;**66**:1901–1914.
100. Pu J, Mintz GS, Brilakis ES, Banerjee S, Abdel-Karim AR, Maini B, Biro S, Lee JB, Stone GW, Weisz G, Maehara A. In vivo characterization of coronary plaques: novel findings from comparing greyscale and virtual histology intravascular ultrasound and near-infrared spectroscopy. *Eur Heart J* 2012;**33**:372–383.
101. Fard AM, Vacas-Jacques P, Hamidi E, Wang H, Carruth RW, Gardecki JA, Tearney GJ. Optical coherence tomography-near infrared spectroscopy system and catheter for intravascular imaging. *Optics Express* 2013;**21**:30849–30858.
102. Li BH, Leung AS, Soong A, Munding CE, Lee H, Thind AS, Munce NR, Wright GA, Rowsell CH, Yang VX, Strauss BH, Foster FS, Courtney BK. Hybrid intravascular ultrasound and optical coherence tomography catheter for imaging of coronary atherosclerosis. *Catheter Cardiovasc Interv* 2013;**81**:494–507.
103. Li J, Li X, Mohar D, Raney A, Jing J, Zhang J, Johnston A, Liang S, Ma T, Shung KK, Mahon S, Brenner M, Narula J, Zhou Q, Patel PM, Chen Z. Integrated IVUS-OCT for real-time imaging of coronary atherosclerosis. *JACC Cardiovasc Imaging* 2014;**7**:101–103.
104. Nadkarni SK, Pierce MC, Park BH, de Boer JF, Whittaker P, Bouma BE, Bressner JE, Halpern E, Houser SL, Tearney GJ. Measurement of collagen and smooth muscle cell content in atherosclerotic plaques using polarization-sensitive optical coherence tomography. *J Am Coll Cardiol* 2007;**49**:1474–1481.
105. Fleming CP, Eckert J, Halpern EF, Gardecki JA, Tearney GJ. Depth resolved detection of lipid using spectroscopic optical coherence tomography. *Biomed Optics Express* 2013;**4**:1269–1284.
106. Liu L, Gardecki JA, Nadkarni SK, Toussaint JD, Yagi Y, Bouma BE, Tearney GJ. Imaging the subcellular structure of human coronary atherosclerosis using micro-optical coherence tomography. *Nat Med* 2011;**17**:1010–1014.
107. Vinegoni C, Botnaru I, Aikawa E, Calfon MA, Iwamoto Y, Folco EJ, Ntziachristos V, Weissleder R, Libby P, Jaffer FA. Indocyanine green enables near-infrared fluorescence imaging of lipid-rich, inflamed atherosclerotic plaques. *Sci Transl Med* 2011;**3**:84ra45.
108. Yoo H, Kim JW, Shishkov M, Namati E, Morse T, Shubochkin R, McCarthy JR, Ntziachristos V, Bouma BE, Jaffer FA, Tearney GJ. Intra-arterial catheter for simultaneous microstructural and molecular imaging in vivo. *Nat Med* 2011;**17**:1680–1684.
109. Lee S, Lee MW, Cho HS, Song JW, Nam HS, Oh DJ, Park K, Oh WY, Yoo H, Kim JW. Fully integrated high-speed intravascular optical coherence tomography/near-infrared fluorescence structural/molecular imaging in vivo using a clinically available near-infrared fluorescence-emitting indocyanine green to detect inflamed lipid-rich atheromata in coronary-sized vessels. *Circ Cardiovasc Interv* 2014;**7**:560–569.
110. Wang H, Gardecki JA, Ughi GJ, Jacques PV, Hamidi E, Tearney GJ. Ex vivo catheter-based imaging of coronary atherosclerosis using multimodality OCT and NIRAF excited at 633 nm. *Biomed Optics Express* 2015;**6**:1363–1375.
111. Wang B, Karpiouk A, Yeager D, Amirian J, Litovsky S, Smalling R, Emelianov S. In vivo intravascular ultrasound-guided photoacoustic imaging of lipid in plaques using an animal model of atherosclerosis. *Ultrasound Med Biol* 2012;**38**:2098–2103.
112. Fatakdwala H, Gorpas D, Bishop JW, Bec J, Ma D, Southard JA, Margulies KB, Marcu L. Fluorescence lifetime imaging combined with conventional intravascular ultrasound for enhanced assessment of atherosclerotic plaques: an ex vivo study in human coronary arteries. *J Cardiovasc Transl Res* 2015;**8**:253–263.
113. Hibi K, Kimura K, Umemura S. Clinical utility and significance of intravascular ultrasound and optical coherence tomography in guiding percutaneous coronary interventions. *Circ J* 2015;**79**:24–33.